

Supporting Information

Dehydrogenative Oxidation of Hydrosilanes Using Gold Nanoparticle Deposited on Citric Acid-Modified Fibrillated Cellulose: Unveiling the Role of Molecular Oxygen

Butsaratip Suwattananuruk,^a Yuta Uetake,^{*a,b} Rise Ichikawa,^c Ryo Toyoshima,^c
Hiroshi Kondoh^c and Hidehiro Sakurai^{*a,b}

^a*Division of Applied Chemistry, Graduate School of Engineering, Osaka University
2-1 Yamadaoka, Suita, Osaka 565-0871, Japan*

^b*Innovative Catalysis Science Division, Institute for Open and Transdisciplinary Research Initiatives (ICS-OTRI),
Osaka University, 2-1 Yamadaoka, Suita, Osaka 565-0871, Japan*

^c*Department of Chemistry, Faculty of Science and Technology, Keio University
Kohoku-ku, Yokohama 223-8522, Japan.*

uetake@chem.eng.osaka-u.ac.jp, hsakurai@chem.eng.osaka-u.ac.jp

Contents

Instrumentations and Chemicals	S3–S4
Optimization of reaction conditions, kinetic studies, and isotope labelling	S5–S10
Computational study	S11–S13
Characterization data	S14
References	S15–16
NMR spectra	S17–S19

Instrumentations and Chemicals

All manipulations of moisture or air-sensitive compounds were performed by standard Schlenk techniques in anhydrous solvents under a nitrogen atmosphere using flame-dried glassware. Reactions were conducted in an EYELA PPS-2511 personal organic synthesizer. Analytical thin-layer chromatography (TLC) was performed on pre-coated silica-gel aluminum sheets (Merck silica gel 60 F254, Cat. No. 1.05554.0001). Preparative thin-layer chromatography (PTLC) was prepared using Wako Wakogel B-5F. Organo Puric- ω water purification system was used to produce Ultrapure water ($18.2 \Omega \text{ cm}^{-1}$). KUBOTA 7780II high-speed refrigerated centrifuge attached with an RS-2504GS swing rotor was used to perform centrifugal ultrafiltration. EYELA FDU-2200 freeze drying system with a 10-station manifold was used for the freeze drying.

^1H NMR (400 MHz) and ^{13}C NMR (100 MHz) spectra were measured on a JEOL JNM-ECZS400 spectrometer at room temperature. Chloroform- d_1 (CDCl_3) was used as a solvent for NMR measurements. Chemical shifts (δ) are given in parts per million (ppm) downfield from the solvent signal (for ^1H NMR: $\text{CHCl}_3 \delta 7.26 \text{ ppm}$; for ^{13}C NMR: $\text{CDCl}_3 \delta 77.0 \text{ ppm}$) as an internal standard with coupling constants (J) in hertz (Hz).

Gas chromatography (GC) analysis was carried out on a Shimadzu GC-2010 using a REATEK Rtx-5MS (30 m, 0.25 mm ID, 0.25 μm df) column and nitrogen as the carrier gas.

Infrared (IR) absorption spectra were measured by the attenuated total reflection (ATR) method on a JASCO FT/IR-4100 Fourier transform IR spectrometer equipped with a JASCO ATR PRO ONE single reflection ATR optical attachment and a diamond crystal plate. The absorption bands were given in wavenumber (cm^{-1}).

JEOL JEM-2100 electron microscope at an accelerating voltage of 200 kV with using a Holey carbon support films coated Cu microgrid (EMJapan, U1003) was used to record transmission electron microscopy (TEM) images. The TEM grid was applied hydrophilic treatment in a glow discharge irradiation chamber before use. Image-J software was used to analyze the generated TEM images, and the expressed mean diameter and standard deviation are based on an average of 300 particles.

Shimadzu ICPS-8100 emission spectrometer was used to perform induced coupling plasma-atomic emission spectroscopy (ICP-AES).

Unless otherwise noted, all reagents purchased from commercial suppliers were used without further purification.

Tetrahydrofuran (THF, dehydrated Super) and *n*-hexane (dehydrated Super) were purchased from Kanto Chemical Co., Inc., and purified by passing through a Glass Contour Ultimate Solvent System (Nikko Hansen & Co. Ltd.) under nitrogen atmosphere.

Tetrachloroauric acid ($\text{HAuCl}_4 \cdot 4\text{H}_2\text{O}$) was purchased from Tanaka kikinzoku Kogyo K. K. Aqueous $\text{HAuCl}_4 \cdot 4\text{H}_2\text{O}$ solution (25 mmol/L) was prepared by dilution with aqueous HCl solution (40 mmol/L). The exact concentration of aqueous HAuCl_4 solution was determined by ICP-AES measurement prior to use. PVP(K-15) (Mw: 10 kDa), sodium borohydride (NaBH_4), hydrochloric acid (ca. 12 mol/L) and cellulose powder (Lot No. MOF2321) were purchased from Nacalai Tesque, Inc.

Triphenylsilane, triphenylsilanol, methyldiphenylsilane, and dimethylphenylsilane were purchased from Tokyo Chemical Industry Co., Ltd.

[^{18}O]Water (≥ 98 atom%) was purchased from Taiyo Nippon Sanso Corp.

Deuterium oxide (D_2O) and chloroform- d_1 (CDCl_3) containing 0.05% tetramethylsilane (TMS) (99.8%D) were purchased from Cambridge Isotope Laboratories, Inc.

Citric acid and ethyl acetate were purchased FUJIFILM Wako Pure Chemical Corp.

Au:PVP,^{1,2} F-CAC,^{3,4} and Au:F-CAC⁵ were prepared according to the literatures.

Optimization of reaction conditions, kinetic studies, and isotope labelling

General procedure for kinetic study of oxidation of hydrosilanes reaction

To a reaction tube equipped with a magnetic stir bar were added Au:F-CAC, triphenylsilane (**1a**, 0.50 mmol), water, and solvent. To the mixture was added *n*-dodecane (57.5 μ L, 0.25 mmol) as an internal standard. The mixture was stirred under an ambient atmosphere. After stirring for a specific period, an aliquot of the reaction mixture was sampled into GC vial and diluted with ethyl acetate. After stirring the mixture vigorously, GC analysis was conducted by using an aliquot of the resulting organic phase.

GC conditions for analyses of the oxidation of **1a**: Constant linear column flow was adjusted to 50 cm s^{-1} . Temperature of the injector and the detector were held at 270 °C. The GC oven temperature program was set as follows: heated from 50 °C to 200 °C at the rate of 12 °C min $^{-1}$, and then heated to 270 °C at the rate of 6 °C min $^{-1}$. Retention times: *n*-dodecane (10.1 min, internal standard), triphenylsilane (19.4 min, **1a**), triphenylsilanol (21.7 min, **2a**).

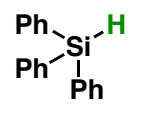
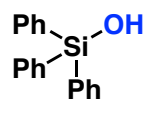
Optimization of reaction conditions

Table S1. Optimization of the amount of H₂O

X	yield (%) ^a
1000	90
400	93
300	88
200	57
100	23

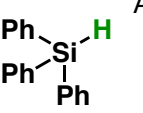
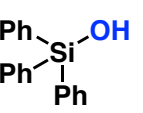
^aDetermined by GC analysis.

Table S2. Optimization of the amount of solvent

	Au:F-CAC (0.01 atom%) H ₂ O (400 mol%) THF (X mL) 27 °C, 5 h, air	
1a (0.5 mmol)		2a
X (mL)		yield (%) ^a
3		99
5		99
10		99

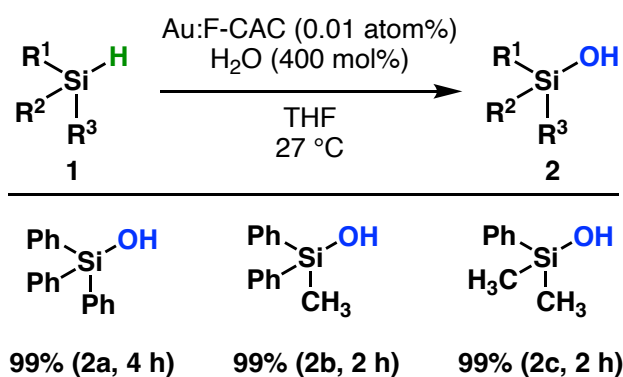
^aDetermined by GC analysis.

Table S3. Optimization of temperature

	Au:F-CAC (0.01 atom%) H ₂ O (400 mol%) THF X °C, 3 h, air	
1a		2a
Temperature (°C)		yield (%) ^a
27		93
50		96
70		90

^aDetermined by GC analysis.

Table S4. Substrate scope



^aDetermined by ¹H NMR analysis.

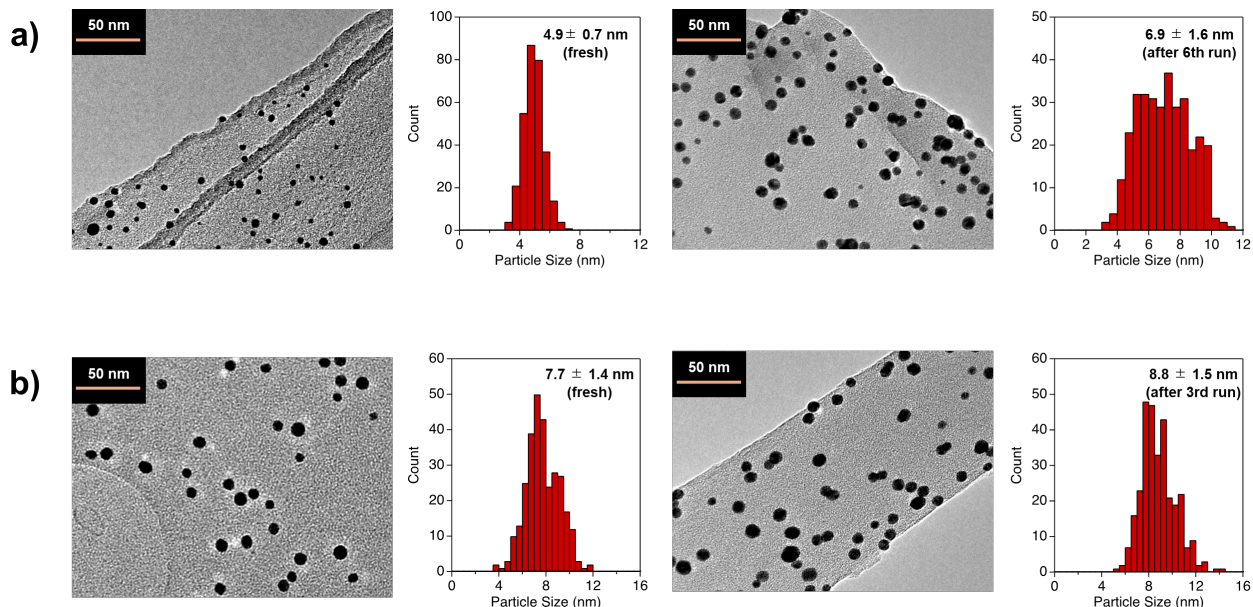


Figure S1. TEM images and size distribution of Au:F-CAC. (a) Au:F-CAC (4.9 nm): fresh (left) and spent catalyst after sixth run (right). (b) Au:F-CAC (7.7 nm): fresh (left) and spent catalyst after third run (right).

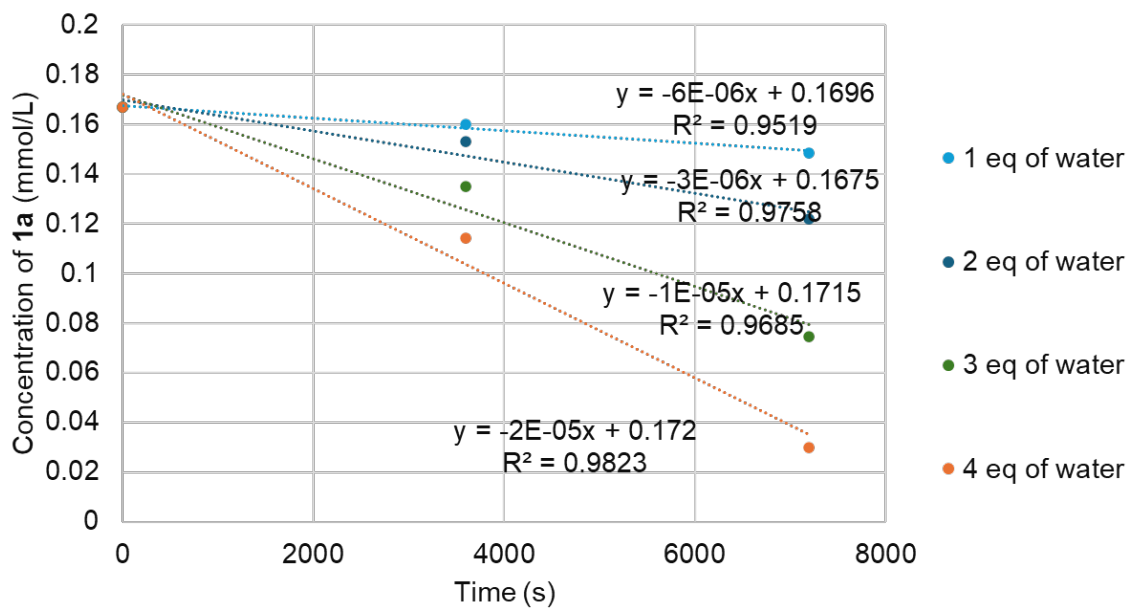


Figure S2. Plots of the concentration of **1a**.

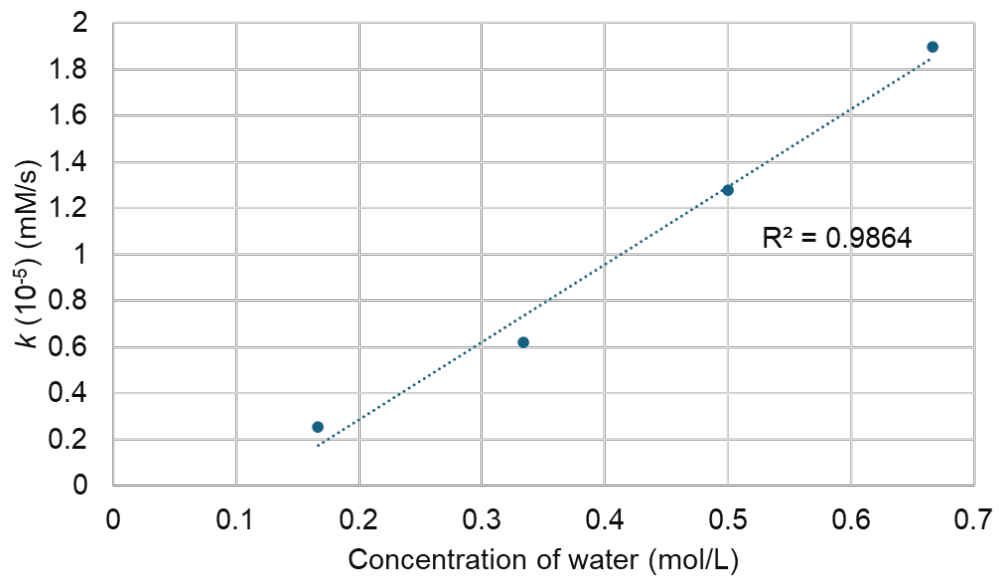


Figure S3. Plots of the reaction rate against the water concentration.

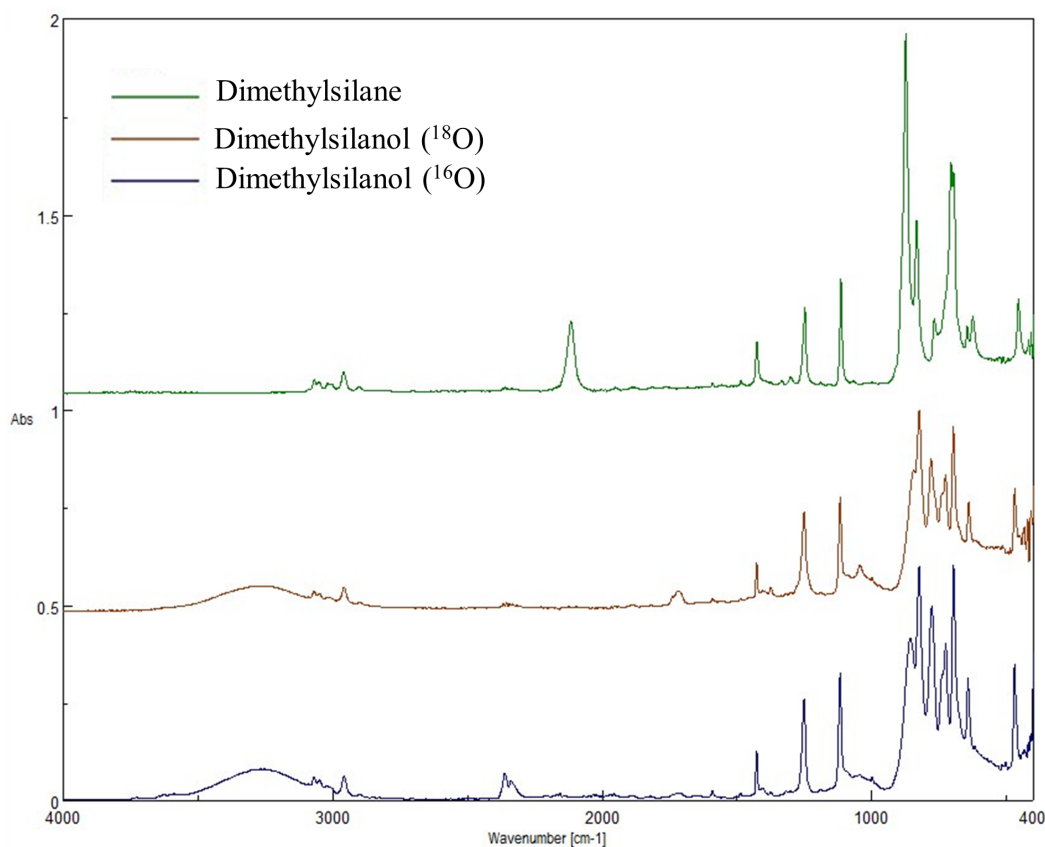


Figure S4: FT-IR spectra of **1a**, **2a**, and [¹⁸O]**2a**

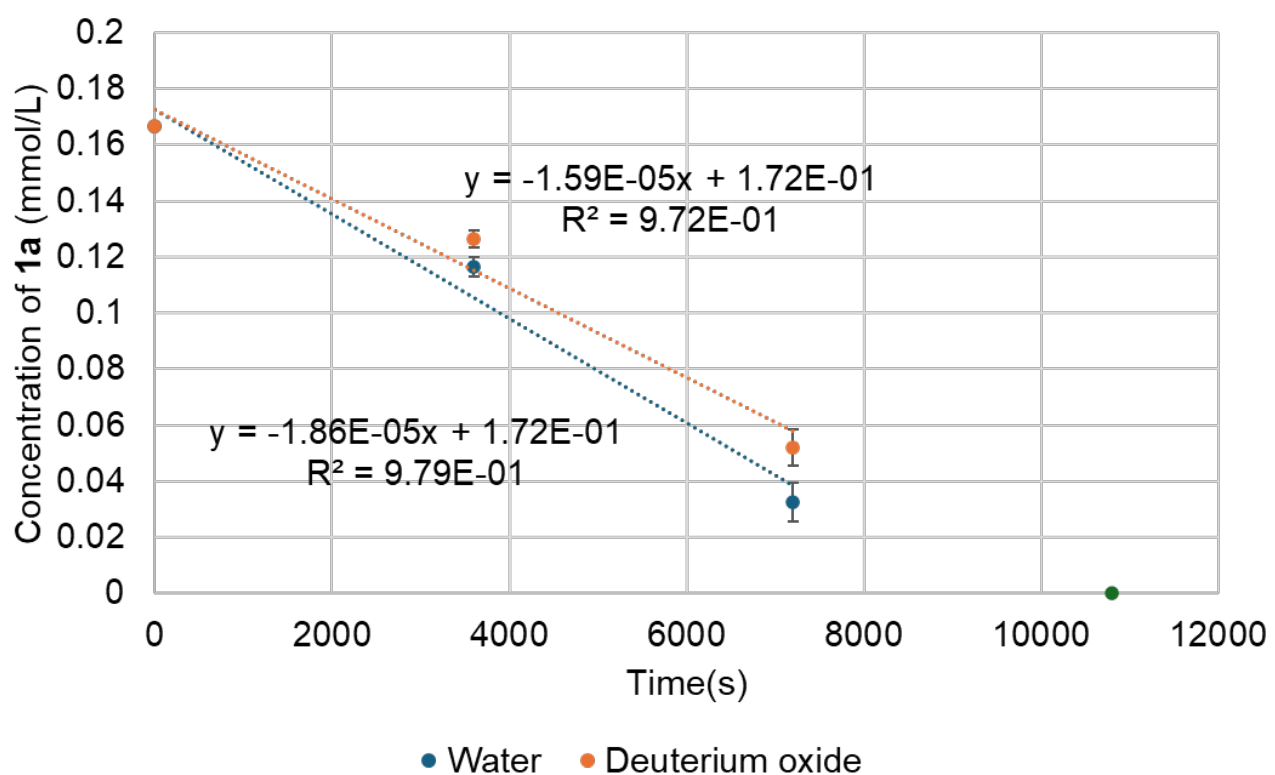


Figure S5: Plots of the concentration of **1a** using H₂O and D₂O.

Table S5. Summary of the reported catalytic activity on dehydrogenative oxidation of dimethylphenylsilane^{6,7}

catalyst	Au loading (mol%)	time (min)	solvent	TOF (h ⁻¹)	reuse (times)	ref.
Au/AlO(OH)	0.1	30	EtOAc	1960	10	8 ^a
AuNPore	1	60	Acetone	10700	5	9 ^b
AuCNT	0.001	360	THF–H ₂ O	9100	5	10 ^a
Au(ONT)	0.05	150	THF	768	4	11 ^a
Au(o-CNTs)	0.1	40	H ₂ O	1477	3	12 ^a
AuHAP	0.83	180	H ₂ O	40	4	13 ^a
MnO ₂ -Au	0.001	10	H ₂ O	590000	10	7 ^a
Au-SiO ₂	0.4	1	THF	59400	5	14 ^b
SBA-PIL-Au	0.4	180	H ₂ O	83	3	15 ^a
AuHAP	0.04	5	Acetone	29711	—	16 ^a
KCC-1-APTS/Au	0.05	1320	THF–H ₂ O	—	10	17
Au-MPBen	52 × 10 ⁻⁶	30	THF	1475	4	18 ^b
Au ₁ /mpg-C ₃ N ₄	0.004	30	Acetone	50200	10	19 ^a
Au/TiO ₂	0.003	30	H ₂ O	—	10	20
Au:F-CAC	0.01	120	THF	7028	5	This work

^aBased on the total gold loading. ^bBased on gold loading on surface.

Computational study

All calculations were performed using Gaussian 16 (revision C.01) program package.²¹ Geometry optimization calculations were carried out by the density functional theory (DFT) method at the B3LYP²² level of theory with the Grimme's dispersion with Becke–Johnson damping (GD3BJ)²³ using 6-31G(d)^{24–27} as a basis set for all atoms in the gas phase. Harmonic frequency calculations were conducted at the same level of theory on the optimized geometries to check all the stationary points as minimum points. The absorption bands of the simulated FT-IR spectra were given in wavenumber (cm^{-1}) with the peak broadening of 4 cm^{-1} .

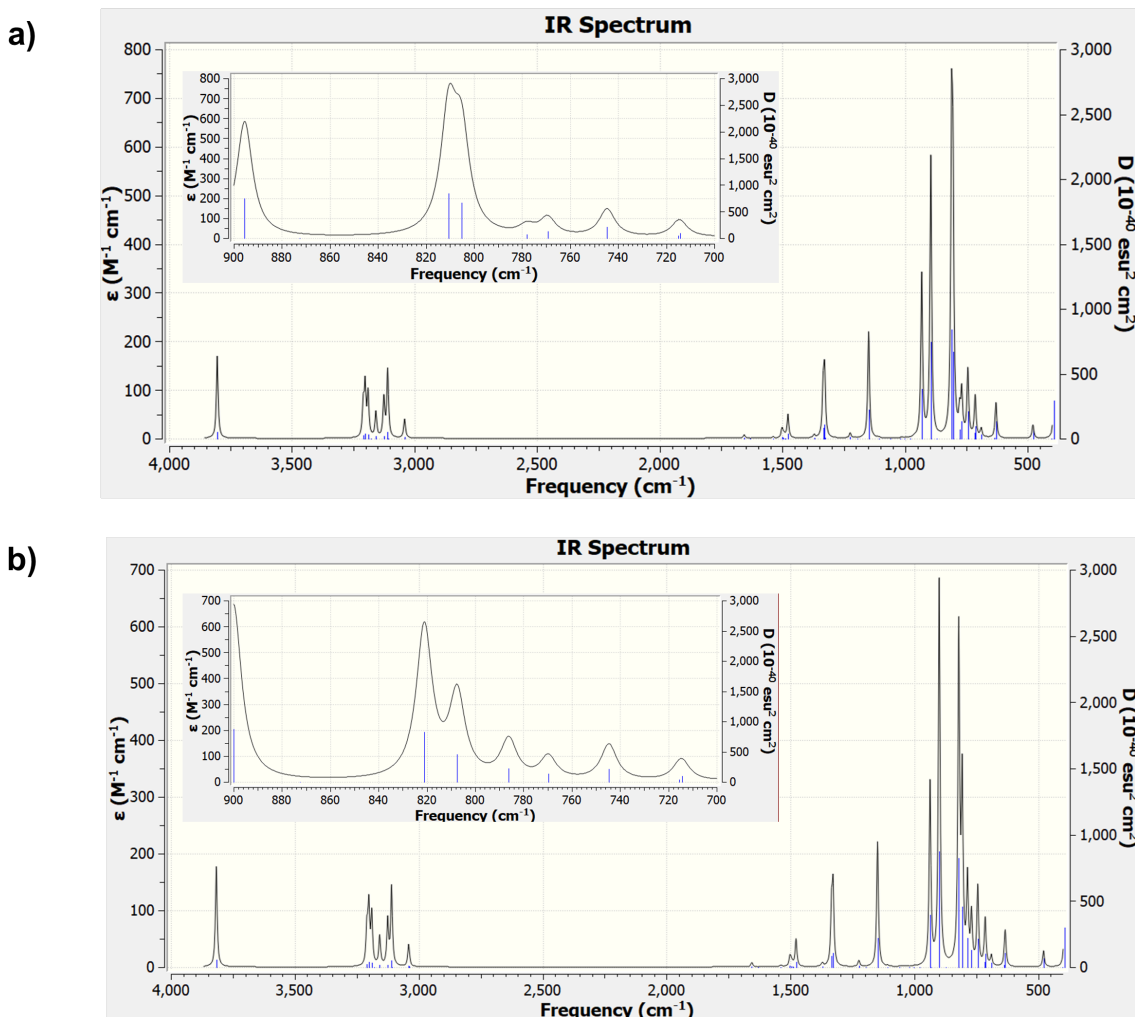


Figure S6: Calculated FT-IR spectra of (a) [¹⁸O]2a and (b) 2a

Optimized coordinates of **2a**

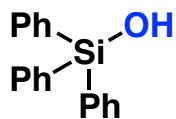
C	-0.19686	-0.28751	-0.05545
C	1.1983	-0.28751	-0.05545
C	1.89583	0.92024	-0.05545
C	1.19818	2.12875	-0.05665
C	-0.19665	2.12867	-0.05713
C	-0.89425	0.92046	-0.05614
H	-0.74662	-1.23983	-0.055
H	1.7478	-1.24003	-0.05414
H	2.99551	0.92032	-0.05482
H	-0.74677	3.08095	-0.05808
H	-1.99385	0.92064	-0.05632
Si	2.16881	3.80847	-0.05676
C	2.52617	4.34895	1.77184
H	3.12409	3.60379	2.25364
H	3.05027	5.2818	1.77209
H	1.60124	4.45936	2.29836
C	1.10428	5.17043	-0.93734
H	1.69251	6.05488	-1.06628
H	0.78588	4.81129	-1.89366
H	0.24731	5.3963	-0.33777
O	3.7515	3.59837	-0.95112
H	4.21306	4.43934	-0.98758

Optimized coordinates of [¹⁸O]2a

C	-0.19686	-0.28751	-0.05545
C	1.1983	-0.28751	-0.05545
C	1.89583	0.92024	-0.05545
C	1.19818	2.12875	-0.05665
C	-0.19665	2.12867	-0.05713
C	-0.89425	0.92046	-0.05614
H	-0.74662	-1.23983	-0.055
H	1.7478	-1.24003	-0.05414
H	2.99551	0.92032	-0.05482
H	-0.74677	3.08095	-0.05808
H	-1.99385	0.92064	-0.05632
Si	2.16881	3.80847	-0.05676
C	2.52617	4.34895	1.77184
H	3.12409	3.60379	2.25364
H	3.05027	5.2818	1.77209
H	1.60124	4.45936	2.29836
C	1.10428	5.17043	-0.93734
H	1.69251	6.05488	-1.06628
H	0.78588	4.81129	-1.89366
H	0.24731	5.3963	-0.33777
O(Iso=18)	3.7515	3.59837	-0.95112
H	4.21306	4.43934	-0.98758

Characterization data

Triphenyl silanol (2a)

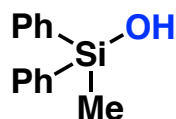


^1H NMR (400 MHz, CDCl_3) δ 7.65–7.62 (m, 6H), 7.47–7.44 (m, 3H), 7.43–7.37 (m, 6H), 2.46 (s, 1H);

^{13}C NMR (100 MHz, CDCl_3) δ 135.10, 134.97, 130.13, 127.92.

The data are consistent with that reported in the literature.²⁸

Methyldiphenylsilanol (2b).

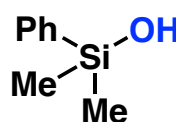


^1H NMR (400 MHz, CDCl_3) δ 7.62–7.01 (m, 4H), 7.44–7.36 (m, 6H), 2.14 (s, 1H), 0.68 (s, 3H);

^{13}C NMR (100 MHz, CDCl_3) δ 137.02, 133.94, 129.91, 127.92, –1.25.

The data are consistent with that reported in the literature.²⁸

Dimethylphenylsilan (2c)



^1H NMR (400 MHz, CDCl_3) δ 7.61–7.59 (m, 2H), 7.42–7.37 (m, 3H), 2.27 (s, 1H), 0.41 (s, 6H);

^{13}C NMR (100 MHz, CDCl_3) δ 139.08, 133.01, 129.59, 127.86, –0.07.

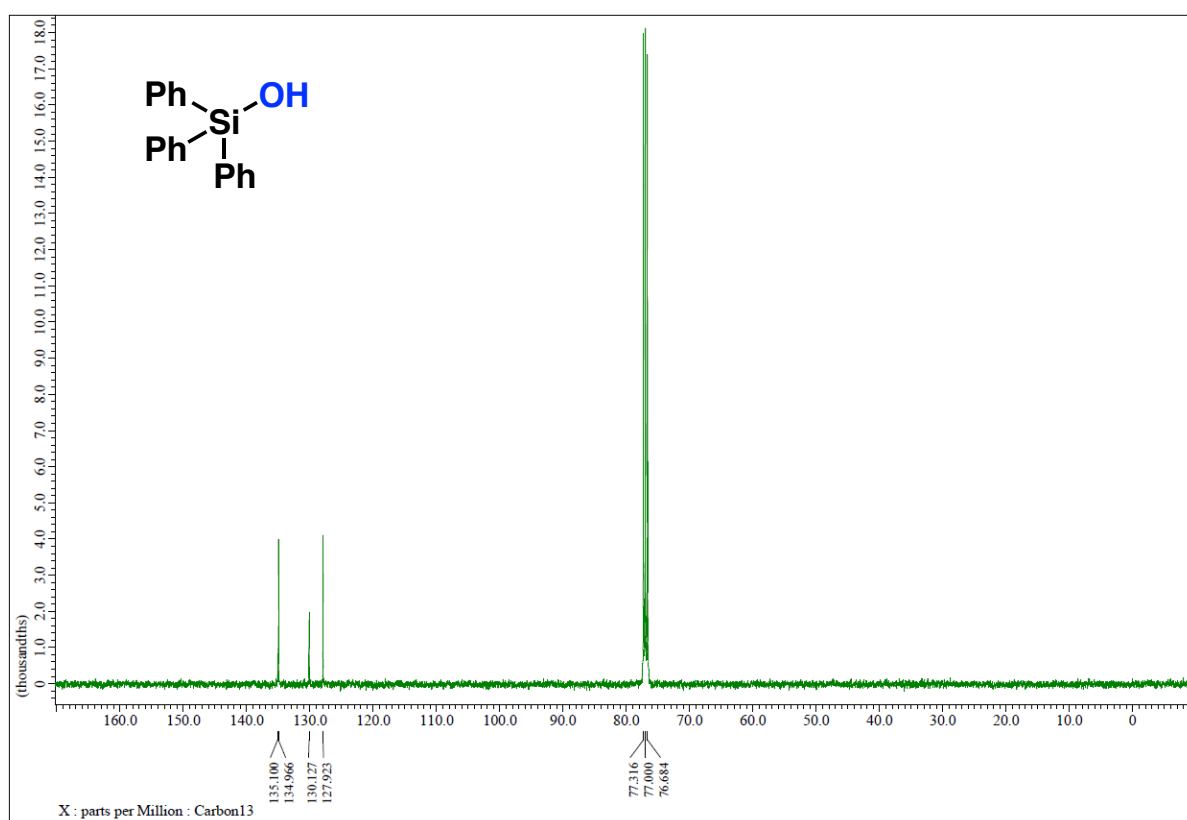
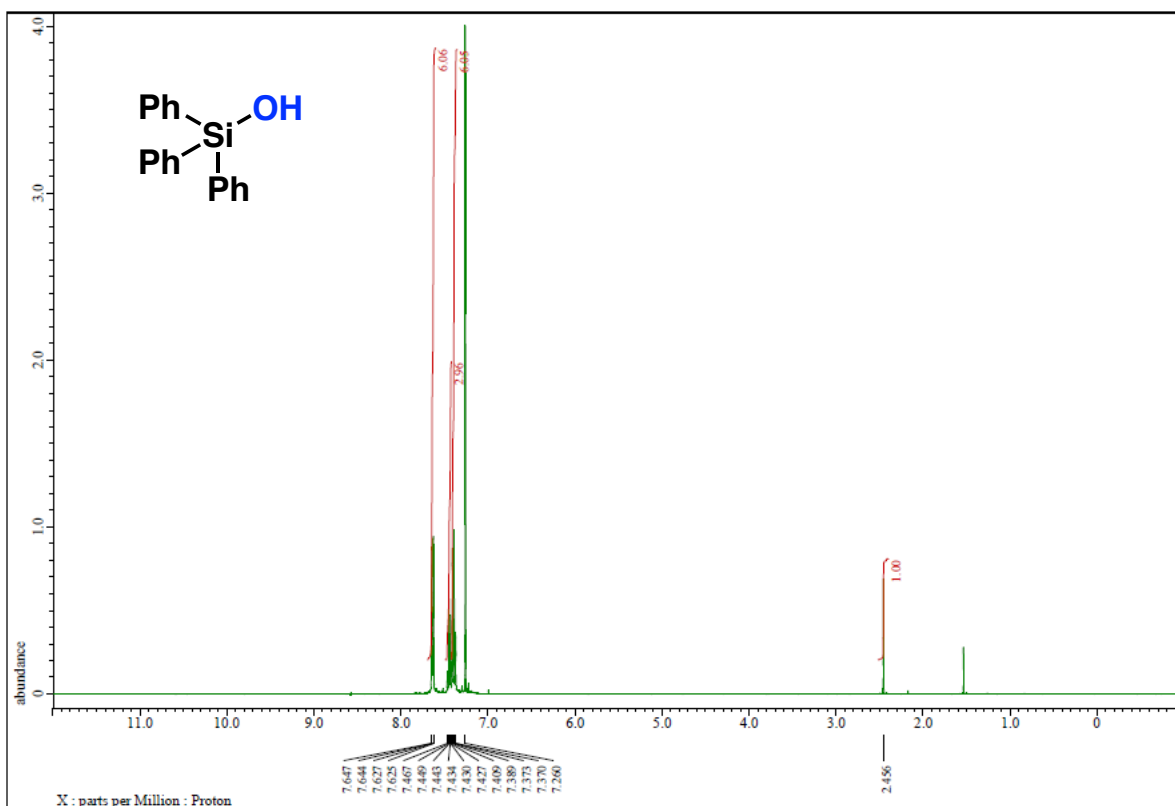
The data are consistent with that reported in the literature.²⁹

References

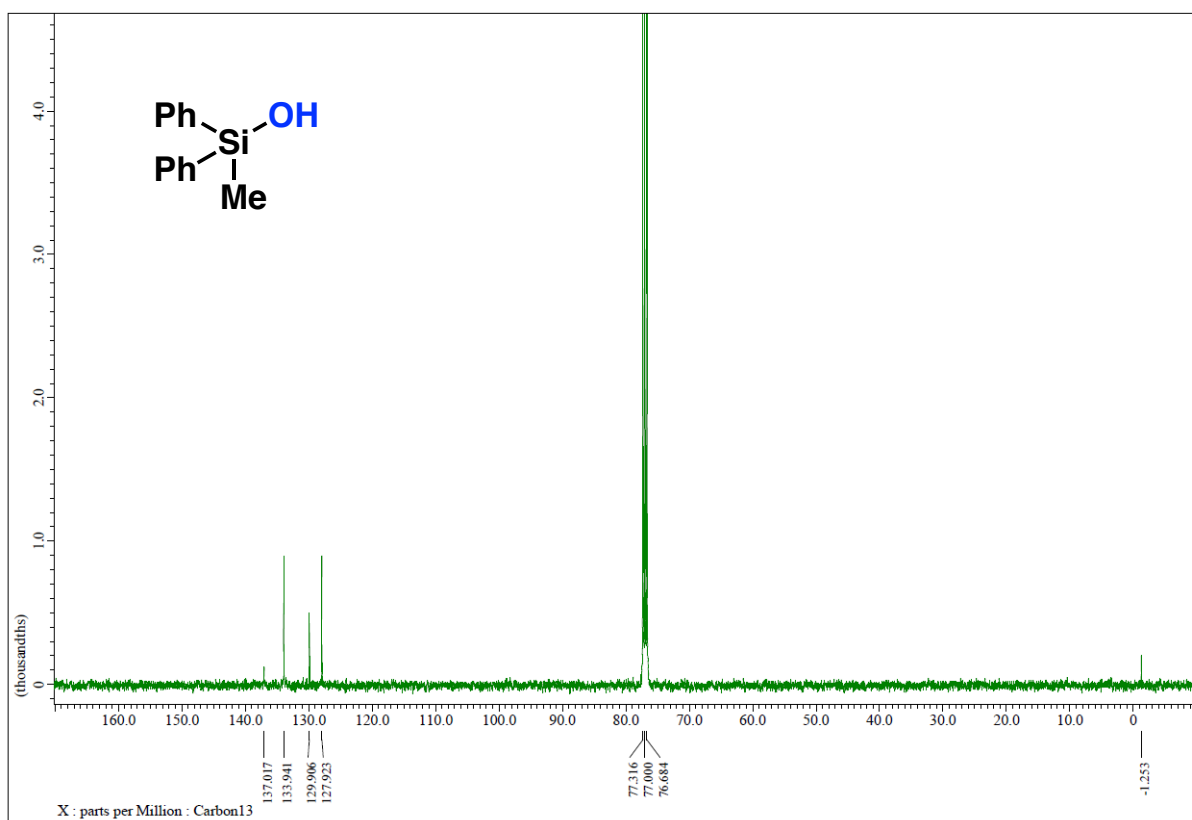
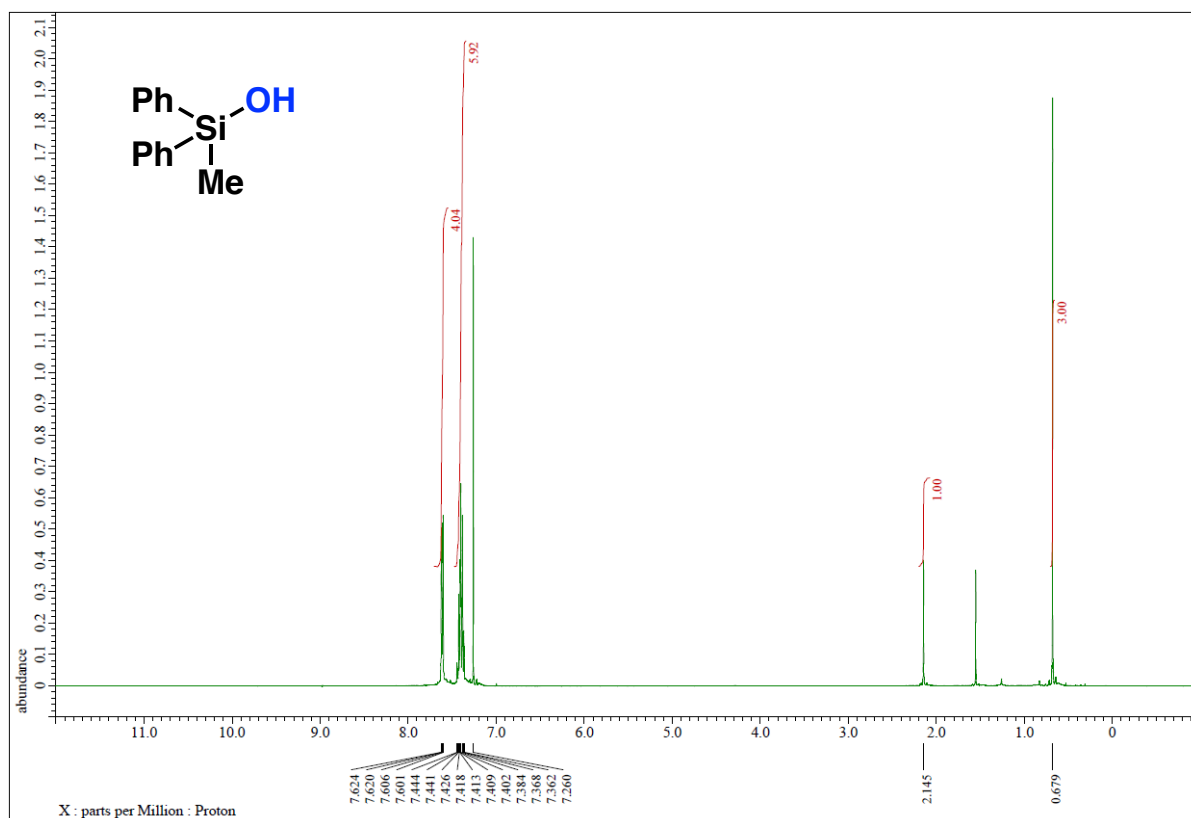
1. H. Tsunoyama, H. Sakurai, Y. Negishi, T. Tsukuda, *J. Am. Chem. Soc.*, 2005, **127**, 9374.
2. H. Tsunoyama, H. Sakurai, T. Tsukuda, *Chem. Phys. Lett.*, 2006, **429**, 528.
3. X. Cui, A. Ozaki, T. Asoh, H. Uyama, *Polym. Degrad. Stab.*, 2020, **175**, 109118.
4. X. Cui, T. Honda, T. Asoh, H. Uyama, *Carbohydr. Polym.*, 2020, **230**, 115662.
5. T. Chutimasakul, Y. Uetake, J. Tantirungrotechai, T. Asoh, H. Uyama, H. Sakurai, *ACS Omega*, 2020, **5**, 33206.
6. W.-S. Huang, H. Xu, H. Yang, L.-W. Xu, *Chem. Eur. J.*, 2024, **30**, e202302458.
7. M. Jeon, J. Han, J. Park, *ChemCatChem*, 2012, **4**, 521.
8. N. Asao, Y. Ishikawa, N. Hatakeyama, Menggenbateera, Y. Yamamoto, M. Chen, W. Zhang, A. Inoue, *Angew. Chem., Int. Ed.*, 2010, **49**, 10093.
9. J. John, E. Gravel, A. Hagège, H. Li, T. Gacoin, E. Doris, *Angew. Chem., Int. Ed.*, 2011, **50**, 7533.
10. T. Mitsudome, A. Noujima, T. Mizugaki, K. Jitsukawa, K. Kaneda, *Chem. Commun.*, 2009, 5302.
11. E. Villemin, E. Gravel, D. V. Jawale, P. Prakash, I. N. N. Namboothiri, E. Doris, *Macromol. Chem. Phys.*, 2015, **216**, 2398.
12. T. Liu, F. Yang, Y. Li, L. Ren, L. Zhang, K. Xu, X. Wang, C. Xu, J. Gao, *J. Mater. Chem. A*, 2014, **2**, 245.
13. A. G. M. da Silva, C. M. Kisukuri, T. S. Rodrigues, E. G. Candido, I. C. de Freitas, A. H. M. da Silva, J. M. Assaf, D. C. Oliveira, L. H. Andrade, P. H. C. Camargo, *Appl. Catal.*, 2016, **184**, 35.
14. W. Li, A. Wang, X. Yang, Y. Huang, T. Zhang, *Chem. Commun.*, 2012, **48**, 9183.
15. L. Ma, W. Leng, Y. Zhao, Y. Gao, H. Duan, *Nanoscale*, 2013, **4**, 6807.
16. Y. Sawama, M. Masuda, N. Yasukawa, R. Nakatani, S. Nishimura, K. Shibata, T. Yamada, Y. Monguchi, H. Suzuka, Y. Takagi, H. Sajiki, *J. Org. Chem.*, 2016, **81**, 4190.
17. M. Dhiman, B. Chalke, V. Polshettiwar, *J. Mater. Chem. A*, 2017, **5**, 1935.
18. R. J. Maya, J. John, R. L. Varma, *Chem. Commun.*, 2016, **52**, 10625.
19. Z. Chen, Q. Zhang, W. Chen, J. Dong, H. Yao, X. Zhang, X. Tong, D. Wang, Q. Peng, C. Chen, W. He, Y. Li, *Adv. Mater.*, 2018, **30**, 1704720.
20. H. Li, L. Chen, P. Duan, W. Zhang, *ACS Sustain. Chem. Eng.*, 2022, **10**, 4642.
21. M. J. Frisch, G. W. Trucks, H. B. Schlegel, G. E. Scuseria, M. A. Robb, J. R. Cheeseman, G. Scalmani, V. Barone, G. A. Petersson, H. Nakatsuji, X. Li, M. Caricato, A. V. Marenich, J. Bloino, B. G. Janesko, R. Gomperts, B. Mennucci, H. P. Hratchian, J. V. Ortiz, A. F. Izmaylov, J. L. Sonnenberg, D. Williams-Young, F. Ding, F. Lipparini, F. Egidi, J. Goings, B. Peng, A. Petrone, T. Henderson, D. Ranasinghe, V. G. Zakrzewski, J. Gao, N. Rega, G. Zheng, W. Liang, M. Hada, M. Ehara, K. Toyota, R. Fukuda, J. Hasegawa, M. Ishida, T. Nakajima, Y. Honda, O. Kitao, H.

- Nakai, T. Vreven, K. Throssell, J. A. Montgomery, Jr., J. E. Peralta, F. Ogliaro, M. J. Bearpark, J. J. Heyd, E. N. Brothers, K. N. Kudin, V. N. Staroverov, T. A. Keith, R. Kobayashi, J. Normand, K. Raghavachari, A. P. Rendell, J. C. Burant, S. S. Iyengar, J. Tomasi, M. Cossi, J. M. Millam, M. Klene, C. Adamo, R. Cammi, J. W. Ochterski, R. L. Martin, K. Morokuma, O. Farkas, J. B. Foresman, and D. J. Fox, Gaussian, Inc., Wallingford CT, 2016.
22. P. J. Stephens, F. J. Devlin, C. F. Chabalowski, M. J. Frisch, *J. Phys. Chem.*, 1994, **98**, 11623.
 23. S. Grimme, S. Ehrlich, L. Goerigk, *J. Comput. Chem.*, 2011, **32**, 1456.
 24. M. M. Franc, W. J. Pietro, W. J. Hehre, J. Binkley, *J. Chem. Phys.*, 1971, **54**, 724.
 25. M. S. Gordon, J. S. Binkley, J. A. Pople, W. J. Pietro, W. J. Hehre, *J. Am. Chem. Soc.*, 1982, **104**, 2797.
 26. P. C. Hariharan, J. A. Pople, *Theor. Chim. Acta*, 1973, **28**, 213.
 27. W. J. Hehre, R. Ditchfield, J. A. Pople, *J. Chem. Phys.*, 1972, **56**, 2257.
 28. P. Lian, K. Wang, H. Liu, R. Li, M. Li, X. Bao, X. Wan, *Org. Lett.*, 2023, **25**, 7984.
 29. I. K. Goncharova, R. S. Tukhvatshin, R. A. Novikov, A. D. Volodin, A. A. Korlyukov, V. G. Lakhtin, A. V. Arzumanyan, *Eur. J. Org. Chem.*, 2022, **35**, e202200871.

^1H NMR (400 MHz) and ^{13}C NMR (100 MHz) spectra of **2a** (CDCl_3)



^1H NMR (400 MHz) and ^{13}C NMR (100 MHz) spectra of **2b** (CDCl_3)



^1H NMR (400 MHz) and ^{13}C NMR (100 MHz) spectra of **2c** (CDCl_3)

